This article was downloaded by:
On: *25 January 2011*
Access details: *Access Details: Free Access*
Publisher *Taylor & Francis*
Informa Ltd Registered in England and Wales Registered Number: 1072954 Registered office: Mortimer House, 37-41 Mortimer Street, London W1T 3JH, UK

Liquid Crystals
Publication details, including instructions for authors and subscription information:
http://www.informaworld.com/smpp/title~content=t713926090

Antiferroelectric liquid crystals with amide linking group positioned at chiral tail

Shune-Long Wu[a]; Zih-Lang Yang[a]; Liang-Jye Yu[b]
[a] Department of Chemical Engineering, Tatung University, Taipei 104, Taiwan [b] Department of Chemistry, Tamkang University, Tamsui, Taipei, 25137 Taiwan

To cite this Article Wu, Shune-Long , Yang, Zih-Lang and Yu, Liang-Jye(2007) 'Antiferroelectric liquid crystals with amide linking group positioned at chiral tail', Liquid Crystals, 34: 10, 1145 — 1149
To link to this Article: DOI: 10.1080/02678290701663738
URL: http://dx.doi.org/10.1080/02678290701663738

PLEASE SCROLL DOWN FOR ARTICLE

Full terms and conditions of use: http://www.informaworld.com/terms-and-conditions-of-access.pdf

This article may be used for research, teaching and private study purposes. Any substantial or systematic reproduction, re-distribution, re-selling, loan or sub-licensing, systematic supply or distribution in any form to anyone is expressly forbidden.

The publisher does not give any warranty express or implied or make any representation that the contents will be complete or accurate or up to date. The accuracy of any instructions, formulae and drug doses should be independently verified with primary sources. The publisher shall not be liable for any loss, actions, claims, proceedings, demand or costs or damages whatsoever or howsoever caused arising directly or indirectly in connection with or arising out of the use of this material.

Liquid Crystals, Vol. 34, No. 10, October 2007, 1145–1149

Taylor & Francis
Taylor & Francis Group

Antiferroelectric liquid crystals with amide linking group positioned at chiral tail

SHUNE-LONG WU*†, ZIH-LANG YANG† and LIANG-JYE YU‡

†Department of Chemical Engineering, Tatung University, Taipei 104, Taiwan
‡Department of Chemistry, Tamkang University, Tamsui, Taipei, 25137 Taiwan

(*Received 15 October 2006; accepted in revised form 29 May 2007*)

A homologous series of chiral liquid crystal compounds, *N*-methyl-*N*-pentyl-(*S*)-2-(6-(4-(4-alkyloxyphenyl)benzoyloxy)-2-naphthyl)propionamide, with an amide linkage in a chiral tail was synthesized and their mesomorphic properties studied. All the materials possessed an antiferroelectric smectic C (SmC_A^*) phase, which was confirmed by observations of microscopic texture, switching current behaviour and electro-optical responses. The spontaneous polarization, P_s, and apparent tilt angle, θ, were also measured. The maximum P_s values are in the range of 173–222 nC cm^{-2}, and the maximum θ values are in the range of 26–30°.

Downloaded At: 15:30 25 January 2011

1. Introduction

The antiferroelectric smectic C (SmC_A^*) phase in chiral liquid crystals, which exhibits a dc threshold, double hysteresis and tristable state properties [1–3], has been considered to have great potential in the field of display technology. Thus, a large number of chiral compounds based on the initial discovered structures of MHPOBC [1] and TFMHPOBC [4] were designed and synthesized for investigation. Subsequently, the correlation between molecular structure and the formation of an antiferroelectric phase has been primarily established [5].

Our previous studies on a homologous series of chiral swallow-tailed amide compounds, DP*n*PBNPA (*n*=9–13; see scheme 1), showed that this type of compounds exhibit a monotropic SmC_A^* phase [6]. This is the first example of chiral amide compounds found to possess an antiferroelectric phase. It is generally acknowledged that the amide linkage in low molecular mass molecules may not be easily conductive to mesomorphism due to hydrogen bonding and/or the high polarization of the amide group leading to ease of crystallization. Therefore, only a few liquid crystal compounds containing an amide linkage have been reported [7–11]. Among these compounds, only one chiral material has been reported to possess monotropic SmA* and unidentified SmX* phases [11].

In order to explore this field further, we designed and synthesized a homologous series of chiral amides, MP*n*PBNPA (*n*=10–14; see scheme 1), with *N*-methyl-*N*-pentylamine as part of chiral amide group. The mesomorphic phases of the compounds were investigated and the physical properties of the antiferroelectric phase, such as the spontaneous polarization and apparent tilt angle, were measured.

2. Experimental

2.1. *Characterization of the chiral materials*

The purity of the final compounds was determined by elemental analysis and the chemical structures were identified by ^{1}H NMR using a Bruker WP100SY FT-NMR spectrometer.

Transition temperatures and phase transition enthalpies were determined by differential scanning calorimetry (DSC) using Perkin-Elmer DSC7 calorimeter at a scanning rate of 5°C min^{-1}. Mesophases were identified by the observation of textures using a Nikon Microphot-FXA optical microscope under cross-polarizers with a Mettler FP-82 hot stage in conjunction with a Mettler FP-90HT heat controller. Compounds were

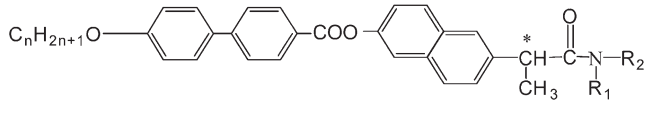

DPnPBNPA (n=9-13) ; $R_1 = R_2 = C_3H_7$

MPnPBNPA (n=10-14) ; $R_1 = CH_3$, $R_2 = C_5H_{11}$

Scheme 1. Chemical structure of the DP*n*PBNPA (*n*=9–13) and MP*n*PBNPA (n=10–14) series.

*Corresponding author. Email: slwu@ttu.edu.tw

Liquid Crystals
ISSN 0267-8292 print/ISSN 1366-5855 online © 2007 Taylor & Francis
http://www.tandf.co.uk/journals
DOI: 10.1080/02678290701663738

filled into 5 μm thick homogeneous aligned cells for the measurement of physical properties. The cells, purchased from Linkam Scientific Instruments Ltd, were fabricated by coating with unidirectional buffed polyimide film. The switching current behaviour and the electro-optical properties in the antiferroelectric phase were measured by the triangle wave method [12].

2.2. *Preparation of chiral compounds*

The chiral compounds were synthesized according to the procedures sketched in scheme 2. The detailed procedures are as follows.

2.2.1. *N*Methyl-*N*-pentyl-(*S*)-2-(6-methoxy-2-naphthyl) propionamide, 2. Oxalyl chloride ($(COCl)_2$, 3.4 ml, 16.94 mmol) was added slowly to (*S*)-2-(6-methoxy-2-naphthyl)propionic acid (2.79 g, 12.1 mmol), **1**, and the resulting solution was refluxed while stirring for 2 h. Excess oxalyl chloride was removed by evaporation under reduced pressure. The crude (*S*)-2-(6-methoxy-2-naphthyl)propionic acid chloride in dichloromethane (5 ml) was added to a solution of *N*-methyl-*N*-pentylamine (1 g, 10 mmol) and triethylamine (TEA, 5 ml) in dichloromethane (10 ml) while stirring under an ice bath. After solids were produced, the mixture was allowed to stand in a refrigerator overnight. The mixture was evaporated to dryness under reduced pressure and the residue was purified by column chromatography over silica gel (70–230 mesh ASTM) using dichloromethane/ethyl acetate (8/2) as eluent. Yield about 75% of white solid. ^{1}H NMR (100 MHz, $CDCl_3$) δ (ppm): 0.76–0.78 (t, 3H, $NCH_2(CH_2)_3C\mathbf{H_3}$), 1.0–1.3 (m, 6H, $NCH_2(C\mathbf{H_2})_3CH_3$), 1.4–1.5 (d, 3H, C*H($C\mathbf{H_3}$)), 2.8–2.9 (d, 3H, $NC\mathbf{H_3}$), 3.0–3.5 (m, 2H, $NC\mathbf{H_2}(CH_2)_3CH_3$), 3.9 (s, 3H, CH_3O), 3.9–4.0 (q, H, ArC*H), 7.1–7.15 (m, 2H, ArH), 7.3–7.4 (t, H, ArH), 7.6–7.65 (t, H, ArH), 7.6–77.7 (t, 2H, ArH).

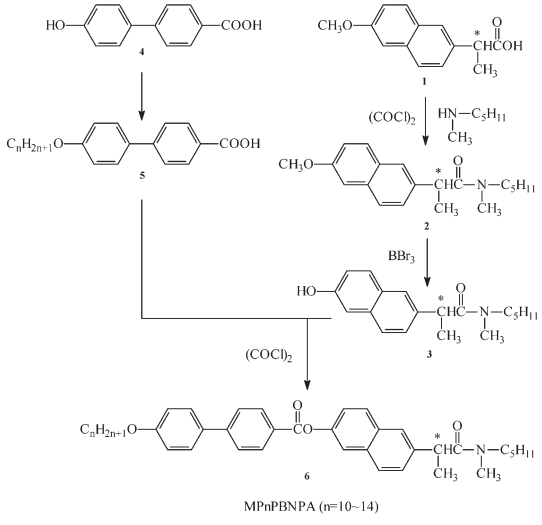

Scheme 2. The schematic synthetic procedures of MP*n*PBNPA (*n*=10–14).

2.1.2. *N*-Methyl-*N*-pentyl-(*S*)-2-(6-hydroxy-2-naphthyl) propionaminde, 3. Compound **2** (2.68 g, 8.55 mmol) dissolved in dry dichloromethane (30 ml) was mixed with boron tribromide (BBr_3, 1.61 ml, 17 mmol) at −20°C. The mixture was stirred at −20°C for 5 min and at 0°C for 40 min. After diluting with dichloromethane (60 ml), the solution was poured into a mixture of saturated ammonium chloride (30 ml) and crushed ice (30 g). The organic layer was separated and washed with brine-ice, dried over anhydrous sodium sulfate ($NaSO_4$), and concentrated in vacuum. Compound **3** was isolated by column chromatography over silica gel (70–230 mesh ASTM) using dichloromethane/ethyl acetate (8/2) as the eluent. The pure compound was collected after purification by the recrystallization from ethanol. Yield 75%. ^{1}H NMR (100 MHz, DMSO-d_6) δ (ppm) 0.6–0.8 (t, 3H, $NCH_2(CH_2)_3C\mathbf{H_3}$), 1.0–1.3 (m, 6H, $NCH_2(C\mathbf{H_2})_3CH_3$), 1.3–1.4 (d, 3H, C*H($C\mathbf{H_3}$)), 2.8–2.9 (d, 3H, $NC\mathbf{H_3}$), 3.0–3.5 (m, 2H, $NC\mathbf{H_2}(CH_2)_3CH_3$), 4.0–4.1 (q, H, ArC*H), 7.0–7.1 (m, 2H, ArH), 7.2–7.3 (d, H, ArH), 7.4–7.7 (m, 3H, ArH), 9.6 (s, H, HO).

2.1.3. *N*-methyl-*N*-pentyl-(*S*)-2-(6-(4-(4′-undecyloxyphenyl)benzoyloxy)-2-naphthyl)propionamide, MP*n*PBNPA (*n*=11). Oxalyl chloride ($(COCl)_2$, 0.27 ml, 1.3 mmol) was added slowly to 4-(4-alkyloxyphenyl)benzoic acid, **5** (*n*=11), (0.47 g, 1.18 mmol) and the resulting solution was heated under reflux while stirring for 2 h. Excess oxalyl chloride was removed by evaporation under reduced pressure. The crude 4-(4-alkyloxyphenyl) benzoic acid chloride in dichloromethane (5 ml) was added to a mixture of compound **4**, (0.33 g, 1.1 mmol) and pyridine (5 ml) in anhydrous dichloromethane (5 ml) with stirring under ice bath. After precipitates were produced, the mixture was allowed to stand in a refrigerator overnight. The mixture was evaporated to dryness under reduced pressure and the residue was purified by column chromatography over silica gel (70–230 mesh ASTM) using dichloromethane/ethyl acetate (10/1) as the eluent. Yield 60%. ^{1}HNMR (100 MHz, $CDCl_3$) δ (ppm): 0.7–0.9 (t, 3H, $C\mathbf{H_3}(CH_2)_8$), 0.7–0.9 (t, 3H, $NCH_2(CH_2)_3C\mathbf{H_3}$), 1.1–1.3 (m, 16H, $CH_3(C\mathbf{H_2})_8$ CH_2CH_2), 1.33–1.44 (m, 6H, $NCH_2(C\mathbf{H_2})_3CH_3$), 1.55 (d, 3H, C*H($C\mathbf{H_3}$)), 1.79–1.84 (q, H, $CH_3(CH_2)_8C\mathbf{H_2}CH_2O$), 2.8–2.9 (d, 3H, NCH_3), 3.0–3.5 (m, 2H, $NC\mathbf{H_2}(CH_2)_3CH_3$), 3.9–4.0 (q, H, ArC*H), 3.99–4.1 (t, 2H, $CH_3(CH_2)_8CH_2C\mathbf{H_2}O$), 7.2–8.3 (m, 14H, ArH). Other

Downloaded At: 15:30 25 January 2011

compounds in the MP*n*PBNPA (*n*=10, 12–14) series were synthesized in the manner described above. Element analysis data for all the target compounds are summarized in table 1.

3. Results and discussion

3.1. *Mesophase properties*

The phase transitions and corresponding phase transition enthalpies of the mesophases of compounds MP*n*PBNPA (*n*=10–14) were measured by DSC. The mesophases were identified by observing microscopic textures under crossed polarizers. The chiral smectic A (SmA*) phase was characterized by the appearance of pseudo-homeotropic textures [13]. The SmC_A* phase appeared in the form of petal texture [14]. The petal texture is one of the characteristics of SmC_A* phase [15], normally observed when the helix of the SmC_A* phase is of a pitch such that the iridescent light in visible region of the spectrum is reflected. It is worth noting that the petal texture selectively reflects coloured light with changing temperature. A green coloured petal texture appeared at 70.6°C, and then changed to a blue coloured petal texture at 68.4°C.

The phase behaviour of MP*n*PBNPA (*n*=10–14) is summarized in table 2 and the phase diagram as a function of the alkyl chain length (*n*) on cooling is plotted in figure 1. It can seen that all compounds exhibit the SmA* and SmC_A* phases. With the exception of compound MP*n*PBNPA (*n*=11), which displayed monotropic SmA* and SmC_A* phases, the rest of compounds displayed enantiotropic SmA* and monotropic SmC_A* phases. Compound MP*n*PBNPA (*n*=11) has the widest temperature range for the SmC_A* phase.

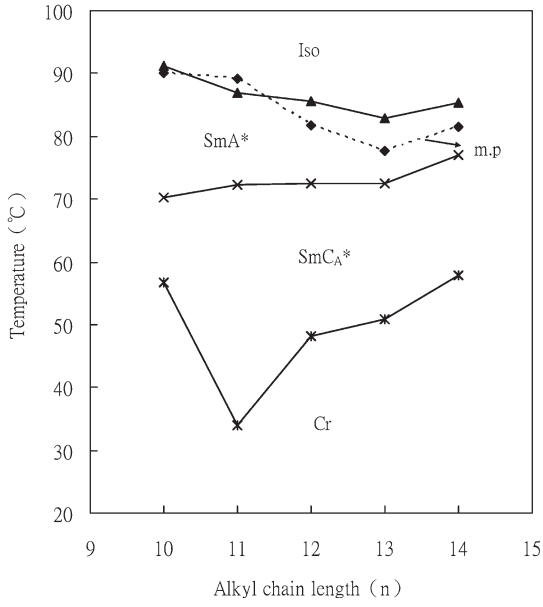

Figure 1. Phase transition temperature versus alkyl chain length, *n*, of MP*n*PBNPA (*n*=10–14) compounds.

Downloaded At: 15:30 25 January 2011

Table 1. Elemental analysis data for MP*n*PBNPA (*n*=10–14) compounds.

	Elemental analysis			
	Theoretical		Experiment	
Compound	C%	H%	C%	H%
MP10PBNPA	79.33	8.40	79.49	8.41
MP11PBNPA	79.47	8.53	78.89	8.50
MP12PBNPA	79.60	8.65	79.97	8.69
MP13PBNPA	79.72	8.77	79.95	8.86
MP14PBNPA	79.84	8.88	79.86	8.89

Table 2. Temperatures (°C) and enthalpies (kJ mol^{-1}, in parentheses) of the phase transitions of MP*n*PBNPA (*n*=10–14) materials measured by DSC at a scanning rate of 5°C min^{-1} on cooling.

Compound	I		SmA*		SmC_A*		Cr	m.p.[a]
MP10PBNPA	•	91.11 (2.33)	•	70.26 (0.06)	•	56.67 (16.39)	•	90.10 (21.06)
MP11PBNPA	•	86.98 (2.04)	•	72.18 (0.26)	•	33.98 (11.56)	•	89.27 (32.26)
MP12PBNPA	•	85.50 (2.82)	•	72.57 (0.35)	•	48.16 (35.73)	•	81.72 (43.81)
MP13PBNPA	•	82.94 (1.97)	•	72.49 (0.30)	•	50.93 (26.84)	•	79.30 (26.84)
MP14PBNPA	•	85.40 (3.11)	•	76.99 (0.39)	•	57.76 (39.17)	•	81.45 (42.42)

[a]m.p. refers to melting point taken from DSC thermogram recorded at heating rate of 5°C min^{-1}. (I=isotropic liquid; Cr=crystal).

3.2. *Electro-optical studies*

In order to confirm the existence of an antiferroelectric phase, the switching current behaviour was used for further investigation. Figure 2 shows the switching current behaviours of compound MP*n*PBNPA (n=11) under a triangle wave with the field frequency of 5 Hz and amplitude of 5 V. There are two switching current peaks at 73°C, as normally observed in the SmC_A* phase [16]. When the temperature is cooled down to 68°C, first peak grows larger than the second one and broadens. Other compounds also displayed similar switching behavior in the antiferroelectric phase.

The electro-optical responses of the compounds were also measured under crossed polarizers where the axes of polarizer and analyzer were parallel and perpendicular to the smectic layer normal in a 5 µm thick homogeneously aligned cell. Figure 3 shows the electro-optical responses of MP*n*PBNPA (n=11) in 5 µm cell under triangle wave and 10 Hz. It shows an ideal double hysteresis loop, a typical characteristic of the SmC_A* phase [17, 18], at 60°C. Figure 4 reveals ideal tristable switching in the antiferroelectric phase [19].

The magnitudes of the spontaneous polarization (P_s) of MP*n*PBNPA (n=11–14) were measured in 5 µm polyimide buffed cells by the triangular wave method [12]; the results are shown in figure 5. The magnitudes of P_s of the MP*n*PBNPA (n=11–14) compounds increased with decreasing temperature and the maximum values are approximately in the range 173–222 nC cm^{-2}.

The apparent tilt angles in the SmC_A* phase for compounds MP*n*PBNPA (n=11–14) were measured as

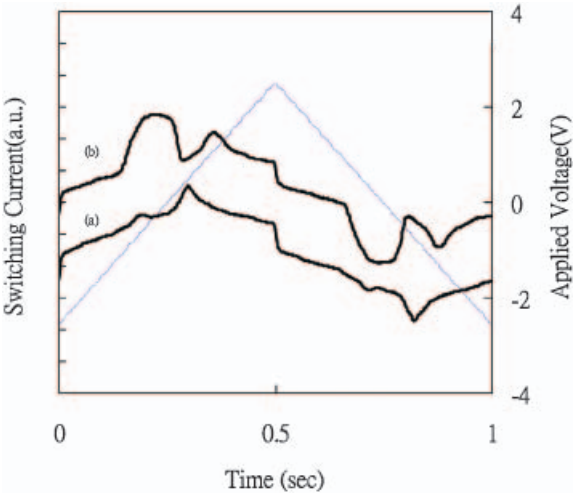

Figure 2. Switching current behaviour of the compound MP*n*-PBNPA (n=11) in the SmC_A* phase at (a) 73°C and (b) 68°C.

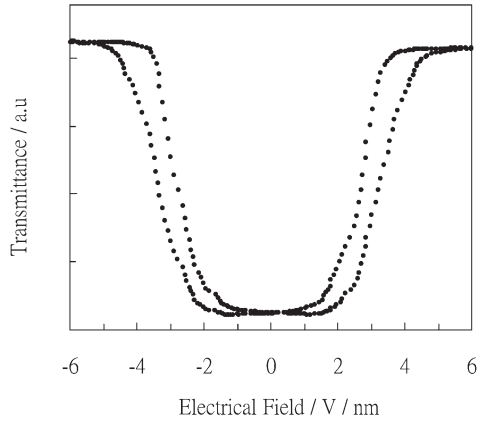

Figure 3. Transmittance versus electrical field obtained at 10 Hz on applying triangular wave to compound MP*n*PBNPA (n=11) in the SmC_A* phase at 60°C.

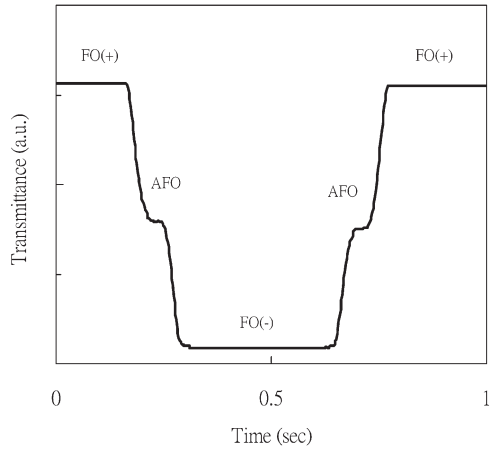

Figure 4. Transmittance versus electrical field obtained for compound MP*n*PBNPA (n=11) at 1 Hz by applying a triangular wave in the SmC_A* phase at 66°C (FO: ferroelectric phase; AFO: antiferroelectric phase).

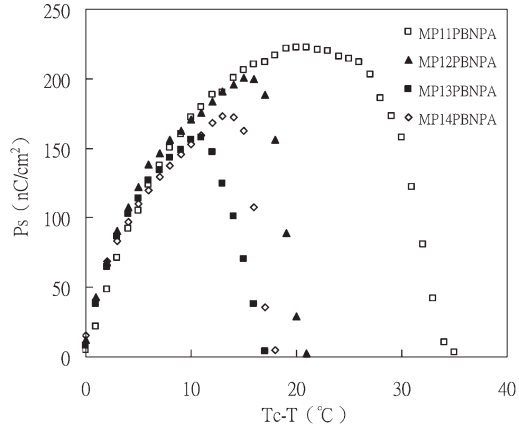

Figure 5. The spontaneous polarization plotted as a function of temperature for MP*n*PBNPA (n=11–14). T_c is the temperature of the SmA*–SmC_A* phase transition.

Downloaded At: 15:30 25 January 2011

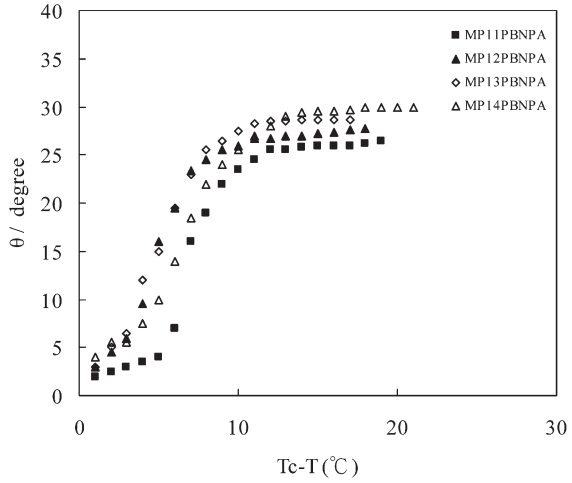

Figure 6. The optical tilt angle plotted as a function of temperature for MP*n*PBNPA (n=11–14). T_c is the temperature of the SmA*–SmC_A* phase transition.

a function of temperature on cooling in a 5 μm homogeneously aligned cell. The plot of tilt angles as the function of temperatures for compounds MP*n*PBNPA (n=11–14) is illustrated in figure 6. The maximum tilt angle increases with increasing aliphatic chain length (n) and the maximum tilt angles are in the range 26–30°.

4. Conclusion

Five chiral amide materials, MP*n*PBNPA (n=10–14), have been synthesized and shown to possess an antiferroelectric SmC_A* phase. The maximum P_s values in the SmC_A* phase of these five compounds are in the range 173–222 nC cm^{-2}, which are approximately twice as large as those previously measured for chiral swallow-tailed amide compounds (maximum P_s=80–87 nC cm^{-2}). This result may be attributed to the damping of the free rotation of chiral centre by the straight pentyl alkyl chain.

Downloaded At: 15:30 25 January 2011

Acknowledgement

The authors are grateful to the financial support of National Science Council of the Republic of China (NSC 94-2216-E-036-008).

References

[1] A.D.L. Chandani, T. Hagiwara, Y. Suzuki, Y. Ouchi, H. Takezoe, A. Fukuda. *Jap. J. appl. Phys.*, **27**, L729 (1988).
[2] A.D.L. Chandani, Y. Ouchi, H. Takezoe, A. Fukuda, K. Terashima, K. Furukawa, A. Kish. *Jap. J. appl. Phys.*, **28**, L1261 (1989).
[3] A. Fukuda, Y. Takanishi, T. Iasozki, K. Ishikawa, H. Takezo. *J. Mater. Chem.*, **4**, 997 (1994).
[4] A. Ikeda, Y. Takanishi, H. Takezeo, A. Fukuda. *Jap. J. appl. Phys.*, **32**, l97 (1993).
[5] J.W. Goodby, A.J. Slaney, C.J. Booth, I. Nishiyama, J.D. Vunk, P. Styring, K.J. Toyne. *Mol. Cryst. liq. Cryst.*, **243**, 231 (1994).
[6] S.-L. Wu, F.-D. Chen. *Liq. Cryst.*, **30**, 991 (2003).
[7] R.A. Vora, R. Gupta. *Mol. Cryst. liq. Cryst.*, **67A**, 251 (1981).
[8] V. Kalyvas, J.E. Mcintyre. *Mol. Cryst. liq. Cryst.*, **80**, 105 (1982).
[9] R.A. Vora, A.K. Prajapati. *Mol. Cryst. liq. Cryst.*, **332**, 329 (1999).
[10] T. Kusumoto, T. Ueda, T. Hiyama, S. Takehara, T. Shoji, M. Oswa, T. Kuriyama, K. Nakamura, T. Fujisawa. *Chem. Lett.*, 523 (1990).
[11] T. Kajitani, S. Kohmato, M. Yamamoto, K. Kishikawa. *Chem. Mater.*, **16**, 2329 (2004).
[12] K. Miyasato, S. Abe, H. Takezoe, A. Fukuda, T. Kuze. *Jap. J. appl. Phys.*, **22**, 661 (1983).
[13] D. Ingo. *Texture of Liquid Crystals*, p. 96, Wiley-VCH Verlag, Weinheim (2003).
[14] S. Inui, N. Iimura, T. Suzuki, H. Iwane, K. Miyachi, Y. Takanishi, A. Fukuda. *J. Mater. Chem.*, **6**, 671 (1996).
[15] I. Nishyama, E. Chin, J.W. Goodby. *J. Mater. Chem.*, **3**, 161 (1993).
[16] A. Fukuda, Y. Takanishi, T. Ioszaki, K. Ishikawa, H. Takezoe. *J. Mater. Chem.*, **4**, 997 (1994).
[17] S. Seomum, T. Gouda, T. Takanishi, K. Ishikawa, H. Takezoe, A. Fukuda. *Liq. Cryst.*, **26**, 151 (1999).
[18] S. Inui, N. Iimura, T. Suzuki, H. Iwane, K. Miyachi, Y. Takanishi, A. Fukuda. *J. Mater. Chem.*, **6**, 671 (1996).
[19] J. Lee, A.D.L. Chandani, K. Itoh, Y. Ouchi, H. Takezoe, A. Fukuda. *Jap. J. appl. Phys.*, **29**, 1122 (1990).